J|A|C|S ARTICLES

Published on Web 11/24/2010

Olefin *Cis*-Dihydroxylation with Bio-Inspired Iron Catalysts. Evidence for an Fe^{II}/Fe^{IV} Catalytic Cycle

Paul D. Oldenburg, Yan Feng, Iweta Pryjomska-Ray, Daniel Ness, and Lawrence Que, Jr.*

Department of Chemistry and Center for Metals in Biocatalysis, University of Minnesota, Minneapolis, Minnesota 55455, United States

Received March 11, 2010; E-mail: larryque@umn.edu

Abstract: Iron(II) complexes of a series of *N*-acylated dipyridin-2-ylmethylamine ligands (R-DPAH) have been investigated as catalysts for the *cis*-dihydroxylation of olefins to model the action of Rieske dioxygenases that catalyze arene *cis*-dihydroxylation. The Rieske dioxygenases have a mononuclear iron active site coordinated to a 2-histidine-1-carboxylate facial triad motif. The R-DPAH ligands are designed to provide a facial *N,N,O*-ligand set that mimics the enzyme active site. The iron(II) complexes of the R-DPAH ligands activate H_2O_2 to effect the oxidation of olefin substrates into *cis*-diol products. As much as 90% of the H_2O_2 oxidant is converted into *cis*-diol, but a large excess of olefin is required to achieve the high conversion efficiency. Reactivity and mechanistic comparisons with the previously characterized Fe(TPA)/H_2O_2 catalyst/oxidant combination (TPA = tris(pyridin-2-ylmethyl)amine) lead us to postulate an Fe^{II}/Fe^{IV} redox cycle for the Fe(R-DPAH) catalysts in which an $Fe^{IV}(OH)_2$ oxidant carries out the *cis*-hydroxylation of olefins. This hypothesis is supported by three sets of observations: (a) the absence of a lag phase in the conversion of the H_2O_2 oxidant into a *cis*-diol product, thereby excluding the prior oxidation of the Fe(II) catalyst to an Fe(III) derivative as established for the Fe(TPA) catalyst; (b) the incorporation of $H_2{}^{18}O$ into the *cis*-diol product, thereby requiring O−O bond cleavage to occur prior to *cis*-diol formation; and (c) the formation of *cis*-diol as the major product of cyclohexene oxidation, rather than the epoxide or allylic alcohol products more commonly observed in metal-catalyzed oxidations of cyclohexene, implicating an oxidant less prone to oxo transfer or H-atom abstraction.

Many iron-based enzymes catalyze the stereospecific oxidation of C=C bonds.[1,2] The most extensively studied of these, the cytochromes P450, have active sites consisting of a heme that is attached to the protein backbone via an iron-coordinating cysteinate residue.[3,4] More recently, nonheme iron enzymes have become better characterized and have been shown to promote novel oxidative chemistry.[2,5] Of particular interest is an enzyme family called the Rieske dioxygenases, which catalyze the *cis*-dihydroxylation of C=C bonds in the biodegradation of arenes in the environment.[6,7] These enzymes have a mononuclear iron center that is ligated by a 2-His-1-carboxylate facial triad,[8,9] a recurring motif among oxygen activating mononuclear nonheme iron enzymes;[10,11] as an example, the active site of naphthalene 1,2-dioxygenase (NDO) is illustrated in Figure 1.[8] There are two potential *cis*-coordination sites on the iron octahedron and these sites are used for the side-on binding of O_2, as demonstrated by X-ray crystallography.[12] On the basis of biochemical studies, this O_2 adduct is proposed to be an iron(III)-peroxo intermediate[13,14] that either attacks a substrate directly or

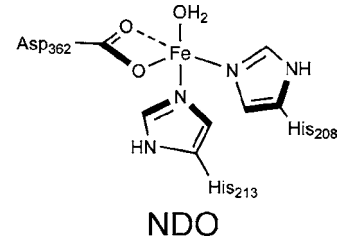

NDO

Figure 1. NDO active site.

(1) Bertini, I.; Gray, H. B.; Stiefel, E. I.; Valentine, J. S., Eds. *Biological Inorganic Chemistry. Structure and Reactivity*; University Science Books: Sausalito, CA, 2007.
(2) Costas, M.; Mehn, M. P.; Jensen, M. P.; Que, L., Jr. *Chem. Rev.* **2004**, *104*, 939–986.
(3) Groves, J. T. In *Cytochrome P450: Structure, Mechanism, and Biochemistry*, 3rd ed.; Ortiz de Montellano, P. R., Ed.; Kluwer Academic/Plenum Publishers: New York, 2005; pp 1−43.
(4) Nam, W.; Ryu, Y. O.; Song, W. J. *J. Biol. Inorg. Chem.* **2004**, *9*, 654–660.
(5) Abu-Omar, M. M.; Loaiza, A.; Hontzeas, N. *Chem. Rev.* **2005**, *105*, 2227–2252.
(6) Gibson, D. T. *Microbial Degradation of Organic Compounds*; Marcel Dekker: New York, 1984.
(7) Gibson, D. T.; Parales, R. E. *Curr. Opin. Biotechnol.* **2000**, *11*, 236–243.
(8) Kauppi, B.; Lee, K.; Carredano, E.; Parales, R. E.; Gibson, D. T.; Eklund, H.; Ramaswamy, S. *Structure* **1998**, *6*, 571–586.
(9) Ferraro, D. J.; Gakhar, L.; Ramaswamy, S. *Biochem. Biophys. Res. Commun.* **2005**, *338*, 175–190.
(10) Hegg, E. L.; Que, L., Jr. *Eur. J. Biochem.* **1997**, *250*, 625–629.
(11) Koehntop, K. D.; Emerson, J. P.; Que, L., Jr. *J. Biol. Inorg. Chem.* **2005**, *10*, 87–93.
(12) Karlsson, A.; Parales, J. V.; Parales, R. E.; Gibson, D. T.; Eklund, H.; Ramaswamy, S. *Science* **2003**, *299*, 1039–1042.
(13) Wolfe, M. D.; Altier, D. J.; Stubna, A.; Popescu, C. V.; Münck, E.; Lipscomb, J. D. *Biochemistry* **2002**, *41*, 9611–9626.
(14) Wolfe, M. D.; Lipscomb, J. D. *J. Biol. Chem.* **2003**, *278*, 829–835.

Scheme 1. Ligands Used for Iron-Based Oxidation Catalysis

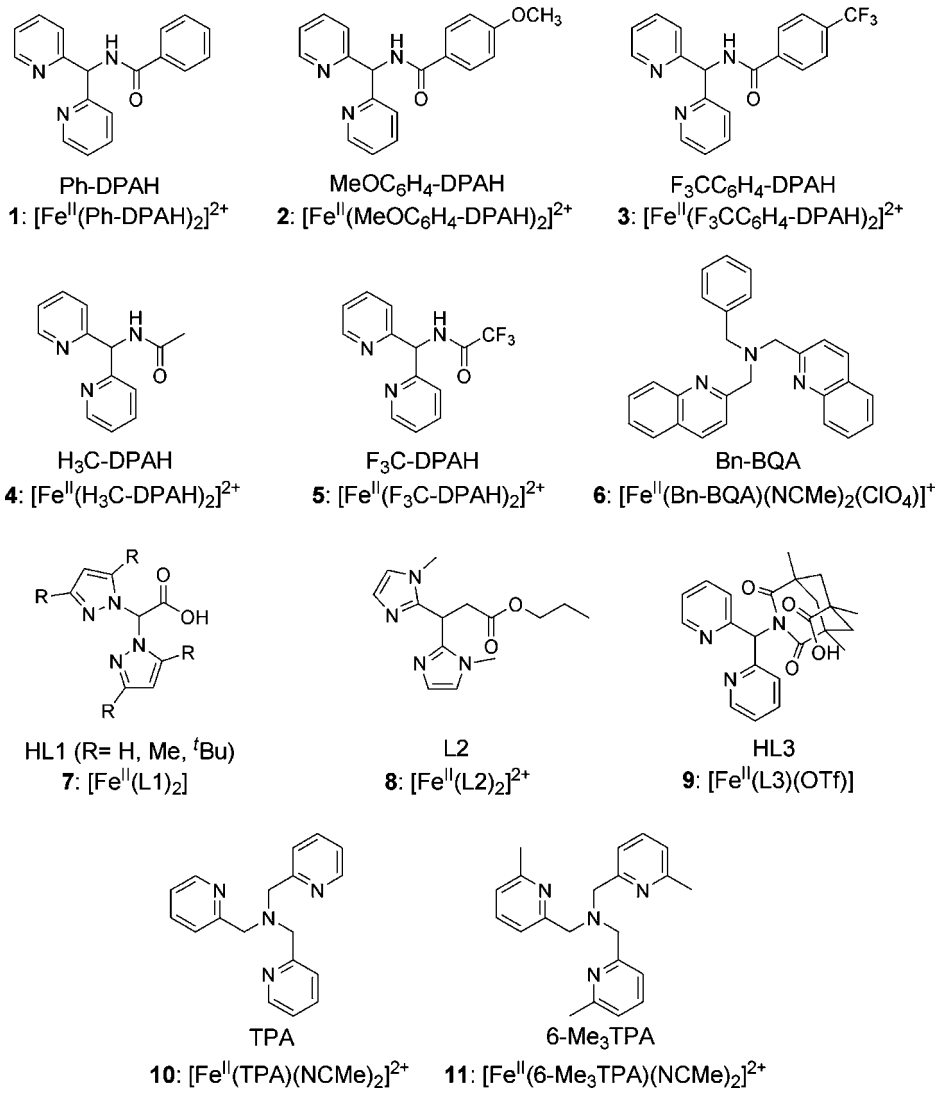

undergoes O−O bond heterolysis to form a HO−Fe^{V}=O species that carries out the *cis*-dihydroxylation.[13,15]

Olefin *cis*-dihydroxylation is an important chemical transformation in both natural product and drug syntheses and typically involves the use of OsO_4.[16,17] The established key role of the mononuclear iron center in the Rieske dioxygenases has thus spurred efforts to design nonheme iron catalysts that mimic the action of these enzymes and develop a more environmentally benign alternative to the osmium-based dihydroxylations. Indeed, examples of such synthetic iron[18−20] as well as manganese catalysts[21,22] have been reported using H_2O_2 as an oxidant. The demonstration of iron-catalyzed *cis*-hydroxylation using H_2O_2 as an oxidant is a particularly significant development, as iron centers typically react with H_2O_2 to generate hydroxyl radicals that give rise to nonspecific oxidation products. The most effective iron complexes thus far are ones that use tetradentate N4 ligands and have two available *cis*-oriented coordination sites that are proposed to facilitate O−O bond cleavage (Scheme 1, complexes **10** and **11**).[18,20] These complexes catalyze both the epoxidation and *cis*-dihydroxylation of olefins by H_2O_2. At present however, the reaction conditions that elicit the best yields of *cis-diols* require (a) syringe-pump introduction of the H_2O_2 oxidant to minimize HO• formation and (b) the use of a large excess of the olefin substrate in order to trap the highly reactive metal-based oxidant responsible for the highly stereoselective *cis*-dihydroxylation. These systems are nevertheless worth investigation to provide a basis for the subsequent development of catalysts suitable for applications in synthetic and pharmaceutical chemistry.

One major difference between the above complexes and the Rieske dioxygenase enzymes is the presence of a carboxylate ligand in the iron coordination environment of the latter. This

(15) Bassan, A.; Blomberg, M. R. A.; Siegbahn, P. E. M. *J. Biol. Inorg. Chem.* **2004**, *9*, 439–452.
(16) Kolb, H. C.; VanNieuwenhze, M. S.; Sharpless, K. B. *Chem. Rev.* **1994**, *94*, 2483–2547.
(17) Ojima, I. *Catalytic Asymmetric Synthesis*, 2nd ed.; Wiley-VCH: New York, 2000.
(18) Chen, K.; Costas, M.; Kim, J.; Tipton, A. K.; Que, L., Jr. *J. Am. Chem. Soc.* **2002**, *124*, 3026–3035.
(19) Costas, M.; Que, L., Jr. *Angew. Chem., Int. Ed.* **2002**, *41*, 2179–2181.
(20) Oldenburg, P. D.; Que, L., Jr. *Catal. Today* **2006**, *117*, 15–21.
(21) De Vos, D. E.; de Wildeman, S.; Sels, B. F.; Grobet, P. J.; Jacobs, P. A. *Angew. Chem., Int. Ed.* **1999**, *38*, 980–983.
(22) de Boer, J. W.; Brinksma, J.; Browne, W. R.; Meetsma, A.; Alsters, P. L.; Hage, R.; Feringa, B. L. *J. Am. Chem. Soc.* **2005**, *127*, 7990–7991.

prompted us and others[23−27] to explore polydentate ligands with a *N*,*N*,*O* donor set to assess how the introduction of an oxygen ligand can affect the performance of the iron catalyst (Scheme 1, species **1**−**5** and **7**−**9**). In our initial efforts, we designed Ph-DPAH,[25] a facial tridentate ligand providing a donor set with two pyridines and an amide carbonyl, and showed that its iron(II) complex **1** catalyzed the *cis*-dihydroxylation of 1-octene, resulting in an unprecedentedly high 76% conversion of the H_2O_2 oxidant to product. This paper reports on further explorations of the catalytic chemistry of **1** and of related complexes (Scheme 1), as well as detailed mechanistic studies that reveal a novel oxidative mechanism involving an Fe^{II}/Fe^{IV} cycle.

Experimental Section

Materials and Synthesis. All reagents were purchased from Aldrich and used as received unless otherwise noted. All olefin substrates were passed over basic alumina immediately prior to use. CH_3CN was distilled from CaH_2. $H_2{}^{18}O_2$ (90% ^{18}O-enriched, 2 wt % solution in $H_2{}^{16}O$) and $H_2{}^{18}O$ (95% ^{18}O enriched) were obtained from ICON Isotopes. The syntheses of the di-(2-pyridyl)methylamine synthon[28] and $[Fe^{II}(OTf)_2{\cdot}2NCCH_3]$[29] have been reported previously.

Syntheses of (Di-(2-pyridyl)methyl)-4-methoxybenzamide (4-MeO-C_6H_4-DPAH) and (Di-(2-pyridyl)methyl)-4-(trifluoromethyl)benzamide (4-F_3C-C_6H_4-DPAH). To a solution containing either 7.8 mmol of 4-methoxybenzoyl chloride or 7.8 mmol of 4-(trifluoromethyl)benzoyl chloride and 1.3 mL of triethylamine in 20 mL of THF was slowly added 1.46 g (7.8 mmol) of di-(2-pyridyl)methylamine at 0 °C. With stirring, this mixture was warmed to 60 °C and heated for 20 min, after which the solution was cooled back to 0 °C and filtered to remove $Et_3N{\cdot}HCl$. THF was removed to afford a cream-colored solid, which was redissolved in CH_2Cl_2 and washed with NaOH. The organic layer was then collected, and the solvent was removed *in vacuo*. Purified products were obtained as white powders after recrystallization from hot MeOH. 4-MeO-C_6H_4-DPAH (70% yield): ^1H NMR ($CDCl_3$, δ ppm from TMS): 8.68 (d, 1H), 8.58 (dm, 2H), 7.94 (dm, 2H), 7.66 (td, 2H), 7.5 (d, 4H), 7.17, (ddd, 2H), 6.39 (d, 1H), 3.86 (s, 3H). ^{13}C NMR ($CDCl_3$): 166.13, 162.28, 159.11, 149.23, 136.91, 129.13, 126.59, 127.52, 122.25, 113.71, 59.32, 55.43. IR (in CD_3CN soln): ν(C═O) 1657 cm^{-1}. 4-F_3C-C_6H_4-DPAH (65% yield): ^1H NMR ($CDCl_3$, δ ppm from TMS): 8.94 (d, 1H), 8.59 (d, 2H), 8.08 (d, 2H), 7.71 (m, 4H), 7.51 (d, 2H), 7.21, (ddd, 2H), 6.42 (d, 1H). ^{13}C NMR ($CDCl_3$): 165.20, 158.31, 149.07, 137.35, 136.97, 132.81, 127.65, 125.44, 122.61, 122.16, 59.16. IR (in CD_3CN soln): ν(C═O) 1668 cm^{-1}.

Synthesis of (Di-(2-pyridyl)methyl)acetamide (H_3C-DPAH). To a solution containing 0.88 g (4.8 mmol) of di-(2-pyridyl)-methylamine in 2 mL of pyridine was added a solution of 0.3 mL (5.2 mmol) of acetic acid in 5 mL of pyridine. This mixture was heated to 80 °C, at which point a solution of 1.7 mL (6.5 mmol) of triphenyl phosphite in 3 mL of pyridine was added over a 2 h period. This mixture was stirred for 24 h at 80 °C, after which the solution was cooled to room temperature and the solvent was removed *in vacuo*, yielding a brown oil. This oil was redissolved into CH_2Cl_2 and washed with 3 × 50 mL fractions of 1 M HCl. The collected aqueous phases were rendered basic (pH ≈ 8) by treatment with sat. $NaHCO_3$ solution. Product was then extracted into CH_2Cl_2 and dried by Na_2SO_4. Solvent was removed *in vacuo*, yielding a light-brown oil. Purified H_3C-DPAH was obtained as a white powder after recrystallization from hot MeOH in 30% yield. ^1H NMR ($CDCl_3$, δ ppm from TMS): 8.55 (d, 2H), 7.91 (d, 1H), 7.64 (td, 2H), 7.43 (d, 2H), 7.16 (d, 2H), 6.22, (d, 1H), 2.15 (s, 3H). ^{13}C NMR ($CDCl_3$): 169.61, 158.90, 149.27, 136.88, 122.51, 122.25, 59.08, 23.44. IR (in CD_3CN soln): ν(C═O) 1677 cm^{-1}.

Synthesis of (Di-(2-pyridyl)methyl)trifluoroacetamide (F_3C-DPAH). To a solution containing 1.15 g (6.2 mmol) of di-(2-pyridyl)methylamine in 3 mL of pyridine was added a solution of 0.52 mL (6.8 mmol) trifluoroacetic acid in 8 mL pyridine. This mixture was heated to 80 °C, at which point a solution of 2.2 mL (8.5 mmol) triphenyl phosphite in 5 mL of pyridine was added over a two-hour period. This mixture was stirred for 24 h at 80 °C, after which the solution was cooled to room temperature and solvent was removed *in vacuo*, yielding a brown oil. Purified F_3C-DPAH was obtained from a silica gel column eluted with a hexanes/ethyl acetate gradient in 58% yield. ^1H NMR ($CDCl_3$, δ ppm from TMS): 9.07 (d, 1H), 8.57 (d, 2H), 7.67 (td, 2H), 7.40 (d, 2H), 7.21 (ddd, 2H), 6.17, (d, 1H). ^{13}C NMR ($CDCl_3$): 156.71, 149.18, 137.15, 122.97, 121.88, 117.69, 58.77. IR (in CD_3CN soln): ν(C═O) 1728 cm^{-1}.

Syntheses of $[Fe^{II}$(4-MeO-C_6H_4-DPAH)$_2](OTf)_2$ (2), $[Fe^{II}$(4-F_3C-C_6H_4-DPAH)$_2](OTf)_2$ (3), $[Fe^{II}(H_3C\text{-DPAH})_2](OTf)_2$ (4), and $[Fe^{II}(F_3C\text{-DPAH})_2](OTf)_2$ (5). In a N_2-containing glovebox, a mixture of the R-DPAH ligand (1.0 mmol) and $Fe^{II}(OTf)_2{\cdot}2NCCH_3$ (0.5 mmol) was stirred for 5 h in 10 mL of CH_3CN. A yellow-green powder formed. Solvent was removed *in vacuo*, and CH_3CN was added until the resulting solid was completely dissolved. For **2** and **3**, vapor diffusion of Et_2O into this solution at −20 °C resulted in the formation of purified **2** after 5 days as bright green, block-shaped single crystals in a 62% yield and purified **3** after 7 days as bright yellow-green, plate-shaped single crystals in a 53% yield, both suitable for X-ray crystallographic analysis. See Supporting Information for details regarding X-ray crystallographic analysis and Tables S1 and S2 for crystal data and structure refinement for **2** and **3**. For **4** and **5**, layering Et_2O over the CH_3CN solution resulted in the formation of purified product after 1 day at −20 °C as a yellow-green powder in 58% yield for **4** and 65% yield for **5**. Characterization of **2**: ESI/MS: *m*/*z* 843 ($[Fe(MeOC_6H_4\text{-DPAH})_2(OTf)]^+$), 524 ($[Fe(MeOC_6H_4\text{-DPAH})(OTf)]^+$), 347 ($[Fe(MeOC_6H_4\text{-DPAH})_2]^{2+}$), 320 ($[(MeOC_6H_4\text{-DPAH})+H]^+$). Anal. Calcd (found) for $C_{40}H_{34}F_6FeN_6O_{10}S_2$: C, 48.40 (48.26); H, 3.45 (3.43); N, 8.47 (8.53); F, 11.48 (11.54). IR (in CD_3CN soln): ν(C═O) 1618 cm^{-1}. Characterization of **3**: ESI/MS: *m*/*z* 562 ($[Fe(F_3CC_6H_4\text{-DPAH})(OTf)]^+$), 385 ($[Fe(F_3CC_6H_4\text{-DPAH})_2]^{2+}$), 358 ($[(F_3CC_6H_4\text{-DPAH})+H]^+$). Anal. Calcd (found) for $C_{39}H_{27}F_{12}FeN_6O_8S_2$: C, 44.96 (44.50); H, 2.64 (2.59); N, 7.86 (7.85); F, 21.33 (21.32). IR (in CD_3CN sol'n): ν(C═O) 1632 cm^{-1}. Characterization of **4**: ESI/MS: *m*/*z* 659 ($[Fe(H_3C\text{-DPAH})_2(OTf)]^+$), 432 ($[Fe(H_3C\text{-DPAH})(OTf)]^+$), 255 ($[Fe(H_3C\text{-DPAH})_2]^{2+}$), 228 ($[(H_3C\text{-DPAH})+H]^+$). Anal. Calcd (found) for $C_{28}H_{26}F_6FeN_6O_8S_2$: C, 41.60 (41.72); H, 3.24 (3.14); N, 10.39 (10.50); F, 14.10 (14.35). IR (in CD_3CN soln): ν(C═O) 1630 cm^{-1}. Characterization of **5**: ESI/MS: *m*/*z* 617 ($[Fe(F_3C\text{-DPAH})_2\text{-H}]^+$), 486 ($[Fe(F_3C\text{-DPA-H})(OTf)]^+$), 377 ($[Fe(F_3C\text{-DPAH})(NCCH_3)\text{-H}]^+$), 304 ($[(F_3C\text{-DPAH})+Na]^+$), 282 ($[(F_3C\text{-DPAH})+H]^+$). Anal. Calcd (found) for $C_{28}H_{20}F_{12}FeN_6O_8S_2{\cdot}H_2O$: C, 36.70 (36.52); H, 2.20 (2.15); N, 9.17 (9.03); F, 24.88 (24.75). IR (in CD_3CN soln): ν(C═O) 1633 cm^{-1}.

Instrumentation. ^1H and ^{13}C NMR spectra were recorded on a Varian Unity 300 or 500 MHz spectrometer at ambient temperature. Chemical shifts (ppm) were referenced to the residual protic solvent peaks. FTIR spectra were obtained with a Thermo Nicolet Avatar 370 FT-IR instrument. X-ray crystallographic analyses were completed by mounting the crystal on a Bruker-AXS platform diffractometer with a CCD area detector and sealed-tube 3-KW

(23) Beck, A.; Weibert, B.; Burzlaff, N. I. *Eur. J. Inorg. Chem.* **2001**, 521–527.
(24) Beck, A.; Barth, A.; Hu1bner, E.; Burzlaff, N. *Inorg. Chem.* **2003**, *42*, 7182–7188.
(25) Oldenburg, P. D.; Shteinman, A. A.; Que, L., Jr. *J. Am. Chem. Soc.* **2005**, *127*, 15672–15673.
(26) Oldenburg, P. D.; Ke, C.-Y.; Tipton, A. A.; Shteinman, A. A.; Que, L., Jr. *Angew. Chem., Int. Ed.* **2006**, *45*, 7975–7978.
(27) Bruijnincx, P. C. A.; Buurmans, I. L. C.; Gosiewska, S.; Moelands, M. A. H.; Lutz, M.; Spek, A. L.; Koten, G. v.; Klein Gebbink, R. J. M. *Chem.—Eur. J.* **2008**, *14*, 1228–1237.
(28) Renz, M.; Hemmert, C.; Meunier, B. *Eur. J. Org. Chem.* **1998**, 1271–1273.
(29) Hagen, K. S. *Inorg. Chem.* **2000**, *39*, 5867–5869.

X-ray generators. High-resolution electrospray mass spectral (ESI-MS) experiments were performed on a Bruker (Billerica, MA) BioTOF II time-of-flight spectrometer. Product analyses from catalysis experiments were performed on a Perkin-Elmer AutoSystem gas chromatograph (AT-1701 column, 30 m) with a flame ionization detector. Gas chromatography/mass spectral analyses were performed on an HP 6890 GC (HP-5 column, 30 m) with an Agilent 5973 mass analyzer. A 4% NH_3/CH_4 mix was used as the ionization gas for chemical ionization analyses.

Reaction Conditions for Catalytic Oxidations. In a typical reaction, 10 equiv of H_2O_2 (diluted from 35% H_2O_2 solution with CH_3CN resulting in a 70 mM solution) were delivered by syringe pump over a period of 5 min at 25 °C in air to a vigorously stirred 3.7 mL solution of 1.3 μmol of iron catalyst and 1000 equiv of olefin substrate in CH_3CN. The final concentrations were 0.35 mM iron catalyst, 3.5 mM H_2O_2, and 0.35 M olefin. The solution was stirred for an additional 60 min after syringe pump addition, after which organic products were esterified by 1 mL of acetic anhydride together with 0.1 mL of 1-methylimidazole and extracted with $CHCl_3$. An internal standard (naphthalene) was added, and the solution was washed with 1 M H_2SO_4, sat. $NaHCO_3$, and H_2O. The organic layer was dried with Na_2SO_4 and subjected to GC analysis. The products were identified by comparison of their GC retention times and GC/MS with those of authentic compounds.

Isotope Labeling Studies. Similar conditions as those described above were used for isotope labeling studies except for the following details. In experiments involving $H_2{}^{18}O$, 1000 equiv of $H_2{}^{18}O$ were added to the commercially available 30% H_2O_2 solution and delivered by syringe pump to the catalyst/substrate solution with the final $H_2{}^{18}O$ concentration equaling 0.35 M. In experiments involving $H_2{}^{18}O_2$, 10 equiv of $H_2{}^{18}O_2$ (diluted by CH_3CN from the commercially available 2% $H_2{}^{18}O_2/H_2O$ solution, which contains a 1:100 molar ratio of $H_2{}^{18}O$ to $H_2{}^{16}O$) were used instead of H_2O_2, with the final $H_2{}^{18}O_2$ concentration equaling 3.5 mM. The diol esterification procedure was the same as that diagrammed above. The data reported either summarize a single reaction or are the average of 2−3 reactions, and the % ^{18}O values reported were calculated based on the ^{18}O-enrichment of the reagents containing the isotope.

Results and Discussion

Structural Analysis. A series of R-DPAH ligands (R = 4-MeO-C_6H_4, 4-F_3C-C_6H_4, CH_3, and CF_3; Scheme 1) can readily be obtained through the acylation of di(2-pyridyl)methylamine. These ligands are variations of the previously reported Ph-DPAH ligand, with each providing a *N,N,O* donor set. The particular R groups were picked to modulate the basicity of the carbonyl oxygen, which in turn may affect the Lewis acidity of the iron center and its interaction with H_2O_2. As with $[Fe^{II}(Ph\text{-}DPAH)_2](OTf)_2$ (**1**), complexes **2**−**5** were synthesized via combination of $[Fe^{II}(OTf)_2(NCMe)_2]$ and 2 equiv of ligand. Single crystals suitable for X-ray analysis were obtained for **2** and **3**, and their structures are shown in Figure 2. Upon iron coordination, the R-DPAH ligands provide a facial array of two pyridines and a carbonyl oxygen in a good approximation of the facial 2-His-1-carboxylate ligand environment found in a number of oxygen activating mononuclear nonheme iron enzymes.[10,11] The structures of **2** and **3** closely resemble that of **1**,[25] with a center of inversion present at each iron center. Diffraction quality crystals could not be obtained for **4** and **5**, but elemental analyses showed a 1:2 metal−ligand stoichiometry as found for **1**−**3**.

Table 1 compares the bond lengths observed in **1**−**3** with those of related complexes **7**,[23,24] **8**,[27] and **9**,[26] as well as those reported for naphthalene dioxygenase (NDO).[8,12] Complexes **7** and **8** are iron(II) complexes with facial *N,N,O* ligand sets developed respectively by Burzlaff (**7**)[23,24] and Klein Gebbink (**8**).[27] Complex **9** differs from **7** and **8** in having an approximately tetragonal *N,N,O,O* ligand set derived from two pyridines and a bidentate carboxylate.[26] The $Fe-N_{pyridine}$ and $Fe-N_{pyrazole}$ bond distances all fall between 2.1 and 2.2 Å, typical of high-spin iron(II) complexes. The $Fe-O_{amide}$ distances of 2.043−2.047 Å observed for **1**−**3** are appreciably shorter than the $Fe-O_{ester}$ distance of **8** but comparable to the $Fe-O_{carboxylate}$ distances found for the complexes of Burzlaff (**7**). This difference reflects a strong interaction between the R-DPAH amide carbonyl oxygen atom with the metal center, comparable to that of a monodentate carboxylate ligand.

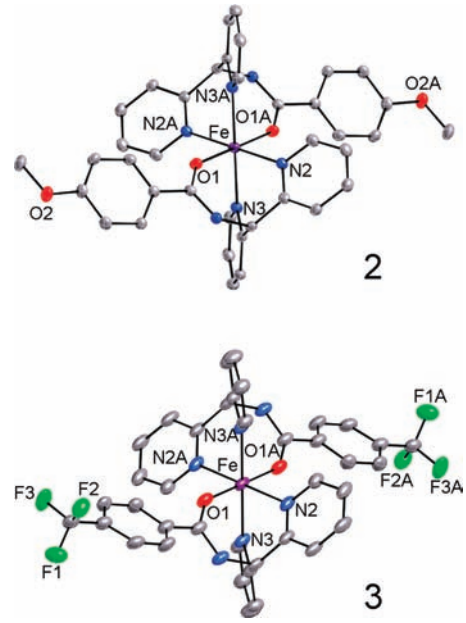

Figure 2. ORTEP plots of complexes **2** and **3** with 50% probability ellipsoids. Hydrogen atoms, counterions, and noncoordinating solvent molecules have been omitted for clarity.

Table 1. Bond Lengths (Å) Observed for the Iron Centers in **1**−**3** and **7**−**9**, As Well As Two Forms of Naphthalene 1,2-Dioxygenase (NDO)

	Fe−N2[a]	Fe−N3[a]	Fe−O1	Fe−O2	ref
1	2.171	2.181	2.043		25
2	2.167(2)	2.187(2)	2.043(2)		This work
3	2.174(2)	2.178(2)	2.047(2)		This work
7	2.169−2.340	2.154−2.353	2.003−2.080		23, 24
8	2.122(2)	2.120(2)	2.228(2)		27
9[b]	2.124	2.137	2.145	2.150	26
NDO[c]	2.0	2.1	2.2	2.6	8
NDO[b]	2.1	2.0	2.3	2.4	14

[a] For NDO, N2 = His208 and N3 = His213. [b] Structure was obtained for related $[Fe^{II}(L1)(Cl)]$ complex. [c] 1NDO.pdb. [d] 1O7G.pdb.

Spectroscopic studies suggest that the complexes remain for the most part intact upon dissolution in CH_3CN but undergo ligand scrambling. ESI-MS analysis of CH_3CN solutions of the complexes show that the $[FeL_2]^{2+}$ species represent the dominant peaks in the spectra. For example for **1**, ions are observed at *m/z* 783 for $\{[Fe(Ph\text{-}DPAH)_2](OTf)\}^+$ and *m/z* 317 for $\{[Fe(Ph\text{-}DPAH)_2]\}^{2+}$, but less intense peaks corresponding to $[Fe(Ph\text{-}DPAH)(OTf)]^+$ (*m/z* 494) and the protonated free ligand (*m/z* 290) can also be detected (Figure 3 top). Similar features are observed for

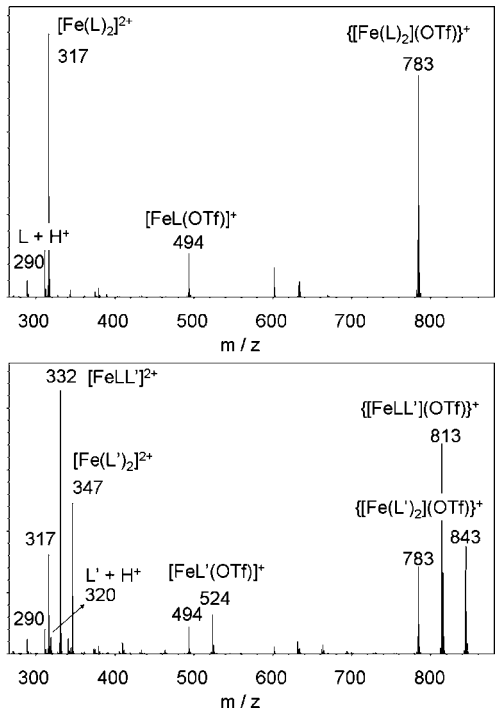

Figure 3. ESI-MS analysis of **1** (0.35 mM) (top) and a mixture of **1** and **2** (bottom) in CH_3CN (L = Ph-DPAH and L′ = 4-MeO-C_6H_4-DPAH).

the other complexes (Figure S1), suggesting the existence of the ligand dissociation equilibrium shown below.

$$[FeL_2]^{2+} \rightleftharpoons [FeL(solv)_x]^{2+} + L$$

In support of this equilibrium, an equimolar mixture of **1** and **2** in CH_3CN affords an ESI-MS spectrum that shows a statistical mixture of $[FeL_2]^{2+}$ ions with the mixed ligand complex $[FeLL']^{2+}$ being the most abundant species in the mixture (Figure 3 bottom). This spectrum is observed immediately upon mixing **1** and **2** in CH_3CN and injecting the solution into the mass spectrometer, showing that ligand scrambling occurs essentially upon dissolution.

FTIR studies shed light on the nature of the species in CH_3CN solution. The Ph-DPAH ligand exhibits an amide $\nu_{C=O}$ at 1662 cm^{-1}. This feature downshifts by 37 cm^{-1} in the solution of the corresponding iron complex **1**, and there is no evidence for the $\nu_{C=O}$ of the free ligand in this solution. Similar results are obtained for **2**−**5**, with respective downshifts of 39, 36, 47, and 95 cm^{-1} observed for these complexes in solution. These downshifts indicate a strong interaction between the ligand amide carbonyl oxygen atoms and the metal center that is also reflected by the relatively short Fe−O distances observed in the crystal structures of **1**−**3**. Only in the case of **5** can some uncoordinated amide be discerned. Taken together, these observations indicate that complexes **1**−**5** in solution retain in large part the 1:2 metal-to-ligand composition found in the crystal structures of **1**−**3**. Furthermore, the ligand dissociation equilibrium postulated above on the basis of the ESI-MS data must lie predominantly to the left in favor of the $[FeL_2]^{2+}$complex.

Catalytic Activities. Table 2 compares the catalytic activities of various complexes in the oxidation of a variety of olefins using H_2O_2 as the oxidant. Also included in the comparison are the results for **10** and **11**, the prototypical complexes in our studies of bio-inspired oxidation catalysis. For these experiments to achieve the desired catalytic outcomes, the substrate olefins must be present in large excess to trap the iron oxidant as soon as it is formed, and the H_2O_2 must be introduced by syringe pump to keep the H_2O_2 concentration low and avoid H_2O_2 disproportionation and generation of hydroxyl radicals. As such, these reaction conditions are not very practical for synthetic chemists. However, these are the only iron catalysts thus far for the conversion of olefins into *cis*-diol products that use H_2O_2 as the oxidant. Thus, the mechanistic insights obtained from this study may be useful for the development of practical catalytic iron chemistry to effect such transformations.

Complexes **1**−**4** represent the first examples of iron complexes that use H_2O_2 as the oxidant and carry out olefin *cis*-dihydroxylation of both electron-rich and electron-poor olefins. Indeed for the oxidation of styrene, 76−94% of the H_2O_2 oxidant was converted to the corresponding *cis*-diol product, and there was ≤1% epoxide product. With 1-octene, *cis*-2-heptene, and dimethyl fumarate as substrates, conversions of the H_2O_2 oxidant for **3** and **4** were comparable to those observed with **1**. Lower conversions (40−56%) were generally found for **2**, where an electron-donating methoxy substituent was introduced on the phenyl ring; however, with styrene as the substrate, **2** exhibited the best catalytic activity, resulting in 94% oxidant conversion to diol. Complex **5**, with the very electron-withdrawing CF_3 group in place of the phenyl, was not a good catalyst and gave low oxidant conversions (4−21%). The trends in the catalytic activities of **1**−**5** suggest that the R-DPAH ligand framework can tolerate a range of R groups, except for the electron-withdrawing trifluoromethyl group adjacent to the amide functionality, which diminishes the performance of **5**. We also investigated the catalytic behavior of related complex **6**,[30] which has one meridional tridentate ligand and three labile binding sites (Scheme 1). Like **1**−**4**, **6** greatly favored *cis*-dihydroxylation over epoxidation but was in general a less efficient catalyst than **1**−**4**. Among all of the iron complexes examined with *cis*-2-heptene and dimethyl fumarate as substrates, >93% of the diol products (and usually 99%) were observed with retention of configuration. These results emphasize that this oxidation is a *cis*-only dihydroxylation and preclude the possibility that epoxidation occurs initially followed by epoxide ring-opening.

Additional experiments were carried out with **1** and **4** to examine their behavior with two other substrates of interest. With cyclohexene as substrate, 10 equiv of H_2O_2 afforded 5.6 equiv of *cis*-cyclohexane-1,2-diol, 0.5 equiv of cyclohexenol, 0.4 equiv of cyclohexenone, and no cyclohexene oxide. The high conversion to the *cis*-diol product is quite remarkable, as cyclohexene oxidation by nonheme iron complexes is most often associated with facile formation of allylic oxidation products.[31−35] On the other hand, no *cis*-dihydroxylation of naphthalene was observed, a different outcome from what was reported for complex **10**.[36]

(30) Kryatov, S. V.; Taktak, S.; Korendovych, I. V.; Rybak-Akimova, E. V.; Kaizer, J.; Torelli, S.; Shan, X.; Mandal, S.; MacMurdo, V.; Mairata i Payeras, A.; Que, L., Jr. *Inorg. Chem.* **2005**, *44*, 85–99.
(31) Guajardo, R. J.; Hudson, S. E.; Brown, S. J.; Mascharak, P. K. *J. Am. Chem. Soc.* **1993**, *115*, 7971–7977.
(32) Kojima, T.; Leising, R. A.; Yan, S.; Que, L., Jr. *J. Am. Chem. Soc.* **1993**, *115*, 11328–11335.
(33) Gosiewska, S.; Lutz, M.; Spek, A. L.; Klein Gebbink, R. J. M. *Inorg. Chim. Acta* **2007**, *360*, 405–417.
(34) Martinho, M.; Banse, F.; Bartoli, J.-F.; Mattioli, T. A.; Battioni, P.; Horner, O.; Bourcier, S.; Girerd, J.-J. *Inorg. Chem.* **2005**, *44*, 9592–9596.
(35) Mukherjee, A.; Martinho, M.; Bominaar, E. L.; Münck, E.; Que, L., Jr. *Angew. Chem., Int. Ed.* **2009**, *48*, 1780–1783.

Table 2. Oxidation of Olefins Catalyzed by Various Iron Complexes with H_2O_2 Oxidant[a]

	1-octene		styrene[b]		*cis*-2-heptene		*tert*-butyl acrylate		dimethyl fumarate	
complex	epox	diol	epox	diol	epox [RC][c]	diol [RC][c]	epox	diol	epox	diol [RC][c]
1	0.1(1)	7.6(3)	0.1(1)	8.0(5)	0.7(1) [57]	4.9(4) [99]	—	5.5(2)	—	5.3(4) [99]
2	<0.1	5.6(4)	<0.1	9.4(3)	0.7(1) [45]	4.1(3) [99]	—	4.5(1)	—	4.0(5) [99]
3	<0.1	7.7(4)	<0.1	7.6(4)	0.5(1) [60]	5.1(3) [99]	—	2.9(4)	—	5.0(4) [99]
4	<0.1	7.7(2)	<0.1	8.9(7)	0.5(1) [44]	5.0(1) [99]	—	5.2(1)	—	5.0(4) [99]
5	0.18(2)	1.3(3)	<0.1	2.1(2)	0.8(1) [43]	0.6(1) [99]	—	0.4(1)	—	0.8(1) [99]
6	<0.1	5.3(3)					—	2.8(3)		
8	1.6	2.7	2.3	1.7	3.1 [84]	3.2 [92]				
9[d]	0.11(1)	0.67(2)			0.37(1) [51]	0.47(5) [96]	—	0.58(4)	—	0.42(4) [99]
10[e]	2.2(1)	5.3(3)	1.7(1)	2.4(1)	1.9(1) [80]	3.0(3) [96]	<0.1[f]	2.6[f]	—	
11[e]	0.3(2)	5.5(2)	0.6(1)	5.2(1)	0.4(1) [35]	4.1(4) [93]	—	6.2[g]	—	5.2[g] [99]

[a] Reaction conditions: 10 equiv H_2O_2 was added by syringe pump over a 5 min period (to minimize H_2O_2 disproportionation) to a solution of catalyst (0.35 mM) and substrate (0.35 M) in CH_3CN (3.7 mL). This solution was stirred for an additional 60 min prior to workup. See Experimental Section for further details. Yields expressed as turnover numbers, TON (μmol of product/μmol of catalyst). [b] Results were obtained under an Ar atmosphere by degassing solutions prior to oxidant introduction so that only a minor amount of the benzaldehyde autoxidation product was observed. See Table S3 for the quantification of this product. [c] %RC: $100 \times (A - B)/(A + B)$, where A = yield of *cis*-diol with retention of configuration and B = yield of epimer. [d] Results from ref 26. [e] Results from ref 18. [f] Result from ref 38. [g] Results from ref 39.

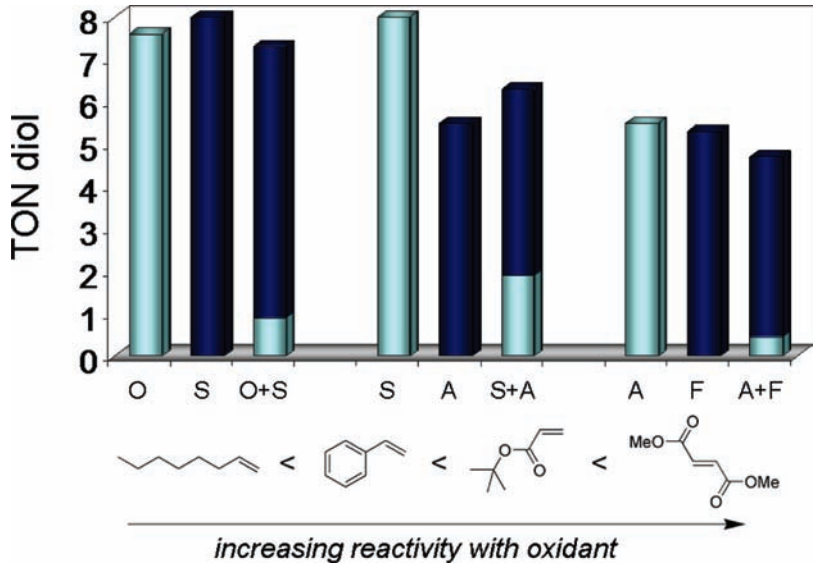

Figure 4. Diol yields resulting from the oxidations of 1-octene (O), styrene (S), *tert*-butyl acrylate (A), and dimethyl fumarate (F), and equimolar mixtures of substrates (O+S, S+A, and A+F) catalyzed by **1** with 10 equiv of H_2O_2 as oxidant.

The longevity of catalyst **1** has been previously investigated by increasing the amount of H_2O_2 introduced,[25] revealing significant deterioration of catalyst activity after the addition of more than 10 equiv of H_2O_2 relative to catalyst. Examination of the ESI-MS data for **1** after a typical catalytic reaction with subsequent treatment with Na_2EDTA to remove iron from the solution shows the presence of peaks arising from species other than the free ligand peaks that indicate ligand oxidation (Figure S2). These peaks correspond to *N*-(dipyridin-2-ylmethylene)benzamide, benzamide, and dipyridin-2-ylmethanone. These products indicate that the Ph-DPAH ligand was oxidized into its imine derivative, which then hydrolyzed into the observed ketone and amide. A similar oxidation of the related *N*-(bis(2-pyridyl)methyl)pyridine-2-carboxamide ligand has been reported.[37] Neither a 1:1:1 mixture of iron(II), benzamide, and dipyridin-2-ylmethanone nor a 1:2 mixture of iron(II) and dipyridin-2-ylmethanone was found to be catalytically active.

Competitive Oxidations. To gather information regarding the interaction of substrate with the oxidant formed in the course of catalysis, substrate competition studies were carried out with pairs of olefin substrates. With **1** as the catalyst, equimolar amounts of two different substrates were oxidized under normal catalytic and workup conditions, and an interesting trend was observed (Figure 4). In individual experiments, **1** catalyzes 1-octene and styrene *cis*-dihydroxylation resulting in 7.6 turnovers of octane-1,2-diol and 8.0 turnovers of phenylethane-1,2-diol. However, when both substrates compete for the active oxidant generated from **1**, the dihydroxylation of styrene was clearly favored, with 6.4 turnovers of phenylethane-1,2-diol and merely 0.9 turnover of octane-1,2-diol. When styrene and *tert*-butyl acrylate compete for the active oxidant, acrylate was favored, with 4.4 turnovers of the diol from acrylate and 1.9 turnovers of styrene diol. Finally, for competition between *tert*-butyl acrylate and dimethyl fumarate, the fumarate was clearly favored by the active oxidant with less than 0.5 turnover resulting in the formation of acrylate diol. Clearly the more electron-deficient olefin is favored in these oxidations. A similar reactivity trend has been previously reported for **11**.[39] The results

(36) Feng, Y.; Ke, C.-y.; Xue, G.; Que, L., Jr. *Chem. Commun.* **2009**, 50–52.
(37) Zhu, S.; Brennessel, W. W.; Harrison, R. G.; Que, L., Jr. *Inorg. Chim. Acta* **2002**, *337*, 32–38.

for both **1** and **11** suggest the active oxidant to be more nucleophilic in nature,[40,41] but the exact nature of this oxidant is not well understood.

A Hammett correlation analysis was also attempted for a series of styrene substrates. Equimolar amounts of styrene and *p*-substituted styrenes were utilized as substrates using **1** as the catalyst under otherwise normal catalytic conditions, and relative yields were analyzed by NMR analysis of the diol products. The substituents of the styrenes changed the diol yields by no more than a factor of 2 with no obvious correlation with σ_p observed (Figure S3).

Isotopic Labeling Studies. ^{18}O labeling experiments have proven useful in previous studies for deducing whether peroxide O−O bond cleavage occurs prior to the attack of substrate by establishing the source of the oxygen atoms incorporated into the product.[18,20,42] As commercially available $H_2{}^{18}O_2$ usually comes as a 2 wt % solution in $H_2{}^{16}O$, every equivalent of $H_2{}^{18}O_2$ added in our labeled studies is accompanied by 100 equiv of $H_2{}^{16}O$. To corroborate these results, complementary labeling experiments with 10 equiv of $H_2{}^{16}O_2$/1000 of equiv $H_2{}^{18}O$ are also carried out. Previous experiments carried out for **10** and **11** with cyclooctene as substrate revealed two distinct labeling patterns.[18] For **10** and related complexes of tetradentate ligands with strong enough ligand fields to support a low-spin iron(II) center in the $[Fe^{II}(L)(NCCH_3)_2]^{2+}$ complexes, the *cis*-diol product incorporated one oxygen atom from H_2O_2 and the other from H_2O (Table 3), results that led us to postulate a water-assisted mechanism for activating the peroxo O−O bond for cleavage. In contrast, for complexes like **11**, which have weaker field ligands due to the presence of α-substituents on the pyridine ligands, both diol oxygens derived exclusively from H_2O_2, thereby requiring a nonwater-assisted pathway for H_2O_2 activation.

Analogous ^{18}O labeling experiments were carried out with **1**−**3**. Figure 5 graphically illustrates the percentages of $^{16}O^{18}O$ and $^{18}O^{18}O$ isotopomers of the diol products obtained from $H_2{}^{18}O_2$ experiments. Table 3 lists the results for all the experiments and demonstrates agreement between the complementary $H_2{}^{18}O$ and $H_2{}^{18}O_2$ experiments. The *cis*-dihydroxylation of dimethyl fumarate by **1**−**3** afforded the *cis*-diol product with both its oxygen atoms derived from H_2O_2. A follow-up labeling experiment carried out with **1** as the catalyst and a 50:50 mixture of $H_2{}^{16}O_2/H_2{}^{18}O_2$ resulted in the generation of a diol product with a 44:7:49 ratio for the $^{16}O^{16}O$, $^{16}O^{18}O$, and $^{18}O^{18}O$ isotopomers, demonstrating that the two diol oxygens incorporated into the fumarate substrate must originate from only one molecule of H_2O_2. (The observed small fraction of the $^{16}O^{18}O$ isotopomer is consistent with the minor amount of $H_2{}^{16}O^{18}O$ present in the 90% enriched $H_2{}^{18}O_2$ solution.) When the labeling experiments were extended to include *tert*-butyl acrylate, styrene, and 1-octene as substrates, some label incorporation from $H_2{}^{18}O$ into their respective diol products was observed (8−29%), and the amount incorporated increased as the olefin substituents became more electron-rich. Because the latter substrates were found to react more slowly than dimethyl fumarate on the basis of the competition experiments presented in Figure 4, the labeling results suggest that there is a competition between the rate of olefin attack by the iron-derived oxidant and the rate at which label scrambling occurs between H_2O_2 and water at the iron center.

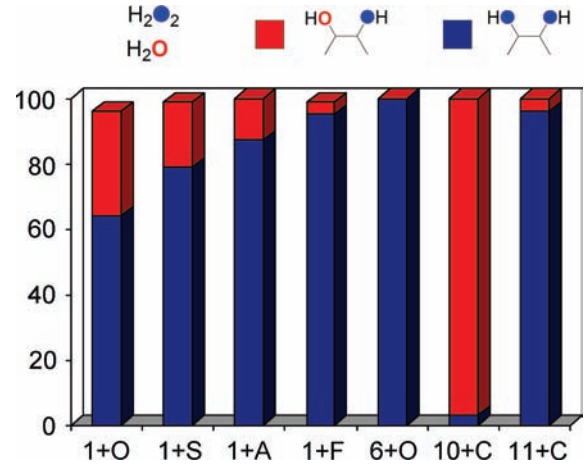

Figure 5. Percentages of diol product with two ^{18}O atoms (blue) and with one ^{18}O atom (red) in olefin *cis*-hydroxylation reactions catalyzed by indicated complexes (0.35 mM) with 10 equiv jof $H_2{}^{18}O_2$ and 1000 equiv of $H_2{}^{16}O$ in CH_3CN solvent at room temperature in the presence of 1000 equiv of olefin. O, S, A, F, and C stand for 1-octene, styrene, *tert*-butyl acrylate, dimethyl fumarate, and cyclooctene, respectively. Data for **10** and **11** obtained from ref 18.

Table 3. Percentages of Isotopomers Found in Diol Products with $H_2{}^{18}O$ or $H_2{}^{18}O_2$ Used As Sources of ^{18}O Atoms in Olefin Oxidations Catalyzed by Indicated Iron Catalysts[a]

		10 $H_2{}^{16}O_2$/1000 $H_2{}^{18}O$		10 $H_2{}^{18}O_2$/1000 $H_2{}^{16}O$		
Catalyst	Substrate	$^{16}O^{16}O$	$^{16}O^{18}O$	$^{16}O^{16}O$	$^{16}O^{18}O$	$^{18}O^{18}O$
1	1-octene	67	29	4	32	64
	styrene	81	18	1	20	79
	tert-butyl acrylate	92	8	0	13	87
	dimethyl fumarate	98	2	1	4	95
2	1-octene	72	26	4	30	65
	styrene	83	17	1	18	81
	tert-butyl acrylate	84	15	1	15	83
	dimethyl fumarate	97	2	3	2	95
3	1-octene	79	18	3	22	74
	styrene	88	12	4	16	80
	tert-butyl acrylate	95	4	2	12	86
	dimethyl fumarate	95	1	0	6	92

[a] Reaction conditions: 3.5 mM H_2O_2 and 0.35 M H_2O delivered by syringe pump to a solution of 0.35 mM catalyst and 0.35 M substrate in CH_3CN (3.7 mL) at room temperature. See Experimental Section for further details.

Additional labeling experiments with **1** as a function of 1-octene (Figure 6) and $H_2{}^{18}O$ (Figure 7) concentration provided additional insight. At a constant $H_2{}^{18}O$ concentration of 0.175 M, the fraction of the *cis*-diol product that incorporated an oxygen atom from water decreased linearly from 33% to 18%, as the concentration of 1-octene increased 20-fold (Figure 6). On the other hand, at a constant 1-octene concentration of 0.35 M, label incorporation from water increased with increasing $H_2{}^{18}O$ concentration and reached a plateau at 0.35 M $H_2{}^{18}O$. This saturation behavior suggests a pre-equilibrium binding of H_2O to the iron center during the catalytic cycle and is supported by the linearity of the double reciprocal plot of these data (Figure 7, inset). These results demonstrate that 1-octene oxidation and water scrambling at the iron center occur at comparable rates.

The 1-octene isotope labeling results for **1**−**3** stand in marked contrast to the near-zero water incorporation into the diol product

(38) Mas-Ballesté, R.; Que, L., Jr. *J. Am. Chem. Soc.* **2007**, *129*, 15964–15972.
(39) Fujita, M.; Costas, M.; Que, L., Jr. *J. Am. Chem. Soc.* **2003**, *125*, 9912–9913.
(40) Wertz, D. L.; Valentine, J. S. *Struct. Bonding (Berlin)* **2000**, *97*, 38–60.
(41) Wada, A.; Ogo, S.; Nagatomo, S.; Kitagawa, T.; Watanabe, Y.; Jitsukawa, K.; Masuda, H. *Inorg. Chem.* **2002**, *41*, 616–618.
(42) Chen, K.; Que, L., Jr. *J. Am. Chem. Soc.* **2001**, *123*, 6327–6337.

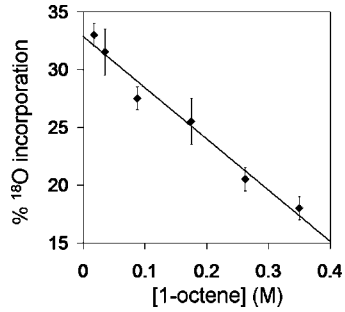

Figure 6. Fraction of ^{18}O-labeled diol in the oxidation of 1-octene catalyzed by **1** with H_2O_2 in the presence of 0.175 M $H_2{}^{18}O$ as a function of the concentration of 1-octene.

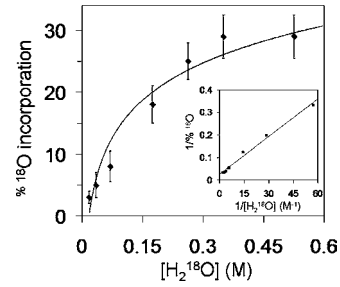

Figure 7. Percent of ^{18}O-labeled diol obtained in the oxidation of 1-octene catalyzed by **1** with H_2O_2 as a function of the concentration of $H_2{}^{18}O$. Inset: double-reciprocal plot.

obtained for **6**. Complex **6** has a meridional tridentate ligand, in place of the facial tridentate ligands used for **1**−**3**. This change in ligand orientation must prevent label scrambling between H_2O_2 and water at the iron center in the case of **6**.

Mechanistic Considerations. The currently favored mechanism for the family of nonheme iron hydrocarbon oxidation catalysts we have investigated is based on extensive work on **10** for which a low-spin Fe^{III}—OOH intermediate can be observed at −40 °C in CH_3CN.[18] This intermediate is proposed to convert to an as yet unobserved HO—Fe^{V}═O oxidant that effects alkane hydroxylation, olefin epoxidation, and olefin *cis*-dihydroxylation.[18,42] (An $S = {}^1/_2$ EPR signal has recently been reported in the reaction of **10** with peracids at −70 °C and is proposed to arise from a putative Fe^{V}═O oxidant,[43] but additional corroboration of the iron(V) oxidation state assignment is needed.) Because the oxygen atom from added $H_2{}^{18}O$ can be incorporated into all the various oxidation products, it is proposed that the H_2O binds to the low-spin Fe^{III}—OOH species and participates in cleaving the O—O bond via a water-assisted mechanism to afford the HO—Fe^{V}═O oxidant where one oxygen atom derives from H_2O. These mechanistic notions are supported by DFT calculations.[44,45]

Much less is known of the peroxide activation mechanism for **11** and related catalysts that favor *cis*-dihydroxylation of olefins. These complexes have weaker field ligands and thus cannot support formation of low-spin iron centers in the catalytic cycle. By analogy to the mechanism proposed for **10** and related catalysts, a high-spin Fe^{III}−OOH species has been proposed in the catalytic cycle, although evidence for such an intermediate

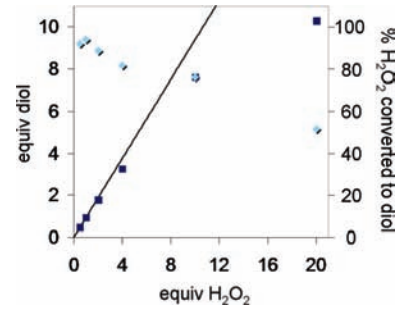

Figure 8. Yield of diol product (■) and percent conversion of H_2O_2 into diol product (◆) as a function of the amount of H_2O_2 added for the oxidation of 1-octene by **1**. Note: the data points at 10 equiv of H_2O_2 are superimposed on each other.

for **11** is lacking.[18,19] However, the corresponding Fe^{III}(6-Me_3-TPA)(OO^tBu) complex has been trapped and characterized spectroscopically to be a high-spin species.[46,47] Because ^{18}O labeling results for **11** do not show any evidence for water incorporation into the *cis*-diol product,[18] the water-assisted mechanism postulated for **10** cannot apply in these cases. It is thus proposed that the peroxide is bound side-on to the iron(III) center as a means of facilitating O−O bond cleavage, and the putative high-spin Fe^{III}-η^2-OOH intermediate is proposed to either attack the substrate directly or undergo O−O bond cleavage to form the HO—Fe^{V}═O oxidant analogous to that proposed for **10**.[18,39]

The R-DPAH family of catalysts provides a unique opportunity to probe the mechanism of the high-spin iron *cis*-dihydroxylation-selective catalysts because of the high yields of *cis*-diol (relative to the H_2O_2 oxidant added) obtained from these reactions. The demonstration that both oxygen atoms of diol are derived from one molecule of H_2O_2 makes it reasonable to propose the initial formation of an Fe/H_2O_2 adduct. Two possible iron-peroxo formulations immediately come to mind: (i) an Fe^{III}−OOH species, like that previously proposed for **11** by extension of the mechanism generally accepted for **10**, or (ii) an $Fe^{II}-O_2H_2$ adduct. Because of the high conversion of H_2O_2 to *cis*-diol for these complexes, it should be possible to distinguish experimentally between these two options by monitoring the percent conversion of H_2O_2 to the diol product as a function of added H_2O_2 equivalents in the oxidation of 1-octene catalyzed by **1** (Figure 8). In the case of option (i), some lag in the production of the *cis*-diol product may be expected due to the requisite initial oxidation of Fe(II) to Fe(III), but such a preoxidation step is not required for option (ii).

As shown in Figure 8, the catalytic behavior of **1** conforms more closely to that expected for option (ii). At low H_2O_2/catalyst ratios, H_2O_2 was converted nearly quantitatively to the diol. For instance, with 0.5 equiv of H_2O_2 added relative to the iron catalyst, 0.46 equiv of diol was formed, amounting to 92% oxidant conversion. Similarly, with 1.0 equiv of H_2O_2 per iron, 0.94 equiv of diol was formed for a 94% conversion of H_2O_2. The percent conversion values decreased with the increasing number of turnovers, 89%, 82%, and 77% with 2, 4, and 10 equiv of H_2O_2, respectively, probably due to some catalyst decomposition. Thus, the first 0.5 equiv of H_2O_2 was not needed to oxidize iron(II) to iron(III) prior to H_2O_2 activation, in contrast

(43) Lyakin, O. Y.; Bryliakov, K. P.; Britovsek, G. J. P.; Talsi, E. P. *J. Am. Chem. Soc.* **2009**, *131*, 10798–10799.
(44) Bassan, A.; Blomberg, M. R. A.; Siegbahn, P. E. M.; Que, L., Jr. *J. Am. Chem. Soc.* **2002**, *124*, 11056–11063.
(45) Bassan, A.; Blomberg, M. R. A.; Siegbahn, P. E. M.; Que, L., Jr. *Chem.—Eur. J.* **2005**, *11*, 692–705.
(46) Zang, Y.; Kim, J.; Dong, Y.; Wilkinson, E. C.; Appelman, E. H.; Que, L., Jr. *J. Am. Chem. Soc.* **1997**, *119*, 4197–4205.
(47) Lehnert, N.; Ho, R. Y. N.; Que, L., Jr.; Solomon, E. I. *J. Am. Chem. Soc.* **2001**, *123*, 12802–12816.

Scheme 2. Mechanistic Overview

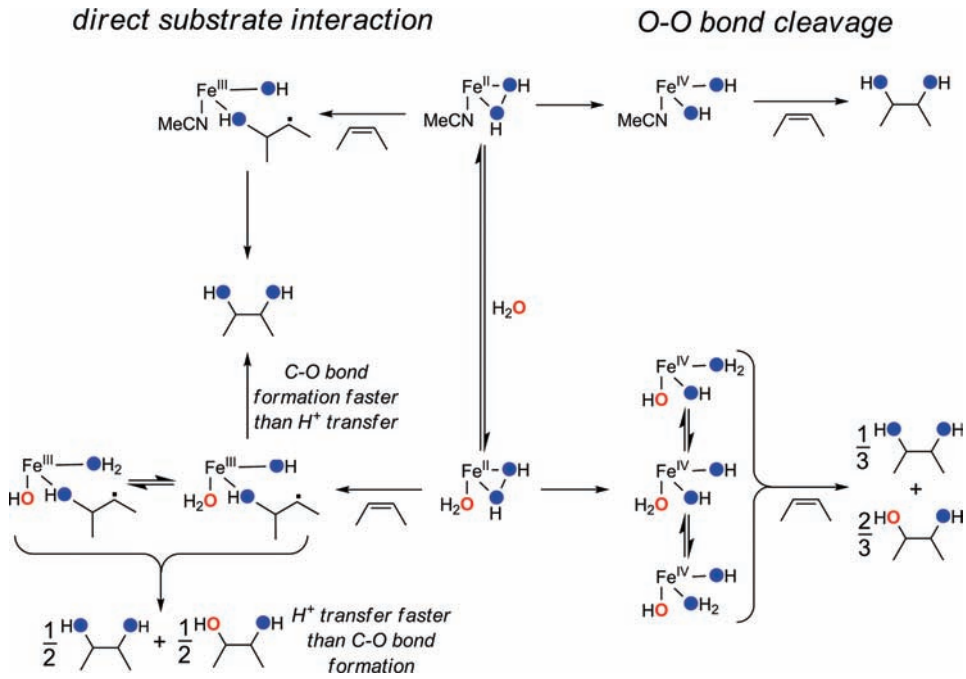

to what was observed for **10**.[18] These results thus unequivocally implicate an initially formed $Fe^{II}-O_2H_2$ adduct as the catalytically relevant iron-peroxo species.

Scheme 2 describes the evolution of this $Fe^{II}-O_2H_2$ species into what we propose to be the active oxidant for olefin *cis*-dihydroxylation derived from the R-DPAH catalysts. The most straightforward way to account for the observation that both diol oxygen atoms derive from one molecule of H_2O_2 is by formation of an $Fe^{II}(\eta^2\text{-}O_2H_2)$ adduct. Formation of such an adduct has been considered and found to be energetically reasonable in computational studies of Fenton chemistry[48,49] and of an iron complex of a tetradentate bispidine ligand that is capable of olefin oxidation catalysis.[50] For the R-DPAH family of catalysts, such an $Fe^{II}(\eta^2\text{-}O_2H_2)$ adduct may be formed either by (a) dissociation of the two carbonyl ligands upon addition of H_2O_2 or (b) loss of one of the R-DPAH ligands. In addition, there must be an additional metal coordination site to bind water to account for the observed label scrambling. For option (a), this would require formation of a seven-coordinate $Fe^{II}(N2)_2(\eta^2\text{-}O_2H_2)(solv)$ intermediate, which may be too sterically crowded. Option (b), on the other hand, is particularly attractive as it can provide three coordination sites on the face of the six-coordinate iron center to allow binding of both a side-on bound H_2O_2 and a water molecule. Evidence that the proposed ligand dissociation equilibrium is established rapidly has been presented in Figure 3. Upon addition, the H_2O_2 would then most likely interact with the 1:1 $[Fe(L)(solv)_x]^{2+}$ species and shift the dissociation equilibrium to the right to form the six-coordinate $Fe^{II}(L)(\eta^2\text{-}O_2H_2)(solv)$ intermediate.

To assess the viability of option (a), we tested whether a 1:2 ratio of $Fe(OTf)_2$ and dipyridin-2-ylmethanone in CH_3CN could catalyze the *cis*-dihydroxylation of 1-octene. However, less than 0.1 equiv of diol was obtained upon addition of 10 equiv of H_2O_2, suggesting that the four-pyridine ligand combination postulated for option (a) is not able to catalyze olefin *cis*-dihydroxylation under the conditions that complexes **1**−**4** can. To assess the viability of option (b), we tested a 1:1 ratio of $Fe(OTf)_2$ and Ph-DPAH and found that this combination was active in catalyzing 1-octene *cis*-dihydroxylation. Addition of 1 equiv of H_2O_2 afforded 0.7(1) TON of the *cis*-diol, while addition of 4 equiv of H_2O_2 resulted in 2.9(2) TON, for about a 73% efficiency in the conversion of H_2O_2 into *cis*-diol, just slightly below that observed for **1** (76%,Table 2 and Figure 8). However, addition of 10 equiv of H_2O_2 afforded only 4.1(2) TON of the *cis*-diol, suggesting significant catalyst deterioration after 3 turnovers. Delaying this outcome may be the role played by the additional Ph-DPAH ligand in **1**. Future work will explore what factors can extend this protective effect to allow more turnovers to be achieved.

Irrespective of which option affords the initial $\eta^2\text{-}O_2H_2$ adduct, the $Fe^{II}(\eta^2\text{-}O_2H_2)(solv)$ intermediate can either play the role of oxidant and attack the olefin directly (Scheme 2, left) or undergo O−O bond cleavage to form an $Fe^{IV}(OH)_2(solv)$ species that reacts with the olefin substrate (Scheme 2, right). In the left branch of Scheme 2, direct attack of the substrate by the $Fe^{II}(\eta^2\text{-}O_2H_2)(solv)$ adduct would result in O−O bond cleavage and formation of the first C−O bond to yield a β-hydroxyethyl radical (S•) that remains coordinated to an $Fe^{III}(OH)(solv)$ moiety. A rapid oxygen rebound must occur to form the second C−O bond and afford the *cis*-diol product with no loss of stereochemistry. In the right branch of Scheme 2, the substrate combines with the dihydroxoiron(IV) moiety to afford the desired product. In either pathway, O−O bond cleavage is proposed to be the rate-determining step.

These two options may be distinguished on the basis of the $H_2{}^{18}O$-labeling results, because the point at which the labeled water can become incorporated into the *cis*-diol product differs. With the addition of excess water, the CH_3CN ligand on the $Fe^{II}(\eta^2\text{-}O_2H_2)(NCCH_3)$ adduct can be displaced by water at least

(48) Ensing, B.; Buda, F.; Blöchl, P.; Baerends, E. J. *Angew. Chem., Int. Ed.* **2001**, *40*, 2893–2895.
(49) Buda, F.; Ensing, B.; Gribnau, M. C. M.; Baerends, E. J. *Chem.—Eur. J.* **2001**, *7*, 2775–2783.
(50) Comba, P.; Rajaraman, G.; Rohwer, H. *Inorg. Chem.* **2007**, *46*, 3826–3838.

Scheme 3

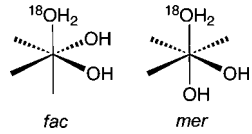

some of the time to generate the $Fe^{II}(\eta^2\text{-}O_2H_2)(OH_2)$ species. In the left branch of Scheme 2, incorporation of a water-derived oxygen atom into the diol product could occur only in the formation of the second C−O bond, via scrambling between the −OH and $-OH_2$ groups by intramolecular proton transfer just prior to the rebound step. If proton transfer proceeded much more quickly than the formation of the second C−O bond, then 50% of the diol product would have one oxygen atom derived from H_2O and the other from H_2O_2. If, however, the rebound is much faster than proton transfer, then both oxygens would derive exclusively from H_2O_2. The fact that 20−30% label incorporation from water is observed suggests that the rates of rebound and proton transfer are comparable. However there is one experimental observation that is inconsistent with this mechanism. Experimental data show that there is an inverse substrate concentration dependence on the extent of label incorporation from water (Figure 6). As label scrambling can occur only after the first C−O bond has already been formed, the extent of label incorporation cannot be affected by the substrate concentration.

On the other hand, the right branch of Scheme 2 is consistent with the observed substrate concentration dependence. In this pathway, the rate-determining cleavage of the η^2-peroxo O−O bond forms an $Fe^{IV}(OH)_2$ oxidant. With ^{18}O-labeled water occupying the solvent binding site, the resulting $Fe^{IV}(OH)_2(H_2{}^{18}O)$ unit can undergo label scrambling prior to attacking the olefin substrate. Intramolecular proton transfer from the bound water to a hydroxo ligand represents a simple mechanism for facile label scrambling, but other plausible mechanisms cannot be excluded. If the rate of scrambling is much faster than the rate of olefin attack, then 33% of diol product should have both oxygen atoms derived from H_2O_2 and 67% should have one oxygen atom each from H_2O and H_2O_2. The fact that the extent of ^{18}O incorporation from labeled water is significantly lower than the predicted 67% suggests a competition between intramolecular label scrambling and intermolecular olefin attack. The extent of label incorporation from $H_2{}^{18}O$ can then be affected by changing the rate of the latter step. This expectation is indeed borne out by the experimental results where label incorporation was observed to decrease with higher olefin concentration (Figure 6) or the use of more reactive olefins (Figure 5).

The R-DPAH complexes described in this paper are the first iron catalysts highly selective for *cis*-dihydroxylation for which label incorporation from $H_2{}^{18}O$ has been observed. We suggest that the observed label scrambling is due to the availability of an additional binding site for water and facilitated by the facial arrangement of the hydroxo and aqua ligands of the $Fe^{IV}(OH)_2(H_2{}^{18}O)$ unit (Scheme 2). The latter point is supported by the observation of no label incorporation from $H_2{}^{18}O$ into the *cis*-diol product from **6** (Figure 5), which is a complex of the tridentate but meridional ligand Bn-BQA (Scheme 1). Extending the mechanism proposed for the R-DPAH complexes to **6** would afford a meridional $Fe^{IV}(OH)_2(H_2{}^{18}O)$ unit (Scheme 3). On the assumption that *cis*-diol formation entails the transfer of two adjacent hydroxo groups to the olefin, then two consecutive proton transfers must occur to incorporate ^{18}O into the product from a meridional $Fe^{IV}(OH)_2(H_2{}^{18}O)$ unit, compared to only one for the facial $Fe^{IV}(OH)_2(H_2{}^{18}O)$ unit.

The experimental results described above lead us to the conclusion that the oxidant produced in the reaction of H_2O_2 with **1**−**4** is a *cis*-$Fe^{IV}(OH)_2$ species, distinct from the isomeric $Fe^{IV}(O)(OH_2)$ species proposed by Baerends in his calculations on the Fenton reaction[49] and from the *cis*-$Fe^{V}(O)(OH)$ oxidant we have proposed for the reaction of H_2O_2 with **10**.[18] The latter two high-valent iron-oxo species would be expected to carry out oxo transfer to olefins and form epoxides, but very little epoxide, if any, is observed in the reactions catalyzed by **1**−**4**. The products observed in the reaction of cyclohexene with **4**/H_2O_2 are quite illustrative in supporting this point, where the dominant product is the *cis*-diol, representing 90% of the products formed. Cyclohexenol and cyclohexenone make up the remaining 10%, and no epoxide was observed. This outcome is distinctly different from oxidations catalyzed by other nonheme iron complexes. For example, in the case of Fe^{II}(cyclam)/H_2O_2, only cyclohexene oxide was observed.[51] On the other hand, allylic oxidation products were the dominant, if not exclusive, products observed for several other complexes,[32−35] demonstrating the susceptibility of the allylic C−H bonds of cyclohexene to oxidative attack. The very low extent of allylic oxidation in the case of the R-DPAH complexes supports the involvement of an oxidant with a much lower hydrogen-atom abstraction capability than is associated with nonheme oxoiron(IV) complexes, which have been shown to be quite facile at carrying out hydrogen-atom abstractions, particularly of allylic C−H bonds.[34,52−54] A recent comparison of oxoiron(IV) and hydroxoiron(IV) species supported by the same tetradentate ligand showed the former to have a 100-fold higher H-atom abstracting ability than the latter.[55] A similar comparison of Mn(IV) complexes also revealed the same trend.[56−58] With a lower hydrogen-atom affinity than its oxoiron(IV) counterpart, the proposed dihydroxoiron(IV) oxidant is consequently well suited to carry out the highly selective *cis*-dihydroxylation of the cyclohexene double bond. Lastly, unlike **10**, **1**−**4** do not catalyze the *cis*-dihydroxylation of the C1−C2 double bond of naphthalene, consistent with the formation of a less powerful oxidant than the $Fe^{V}(O)(OH)$ oxidant associated with **10**.

DFT calculations provide computational precedents for the proposed formation of a dihydroxoiron(IV) species from the reaction of an iron(II) precursor with H_2O_2. In a study of the active species generated in the Fenton reaction, Baerends and co-workers[49] found that $[Fe^{IV}(OH)_2(OH_2)_4]^{2+}$ was the initial high-valent species formed in the reaction of $[Fe^{II}(OH_2)_6]^{2+}$ and H_2O_2, which then isomerized to $[Fe^{IV}(O)(OH_2)_5]^{2+}$ by proton transfer. Comba and co-workers[50] investigated various pathways leading to the formation of high-valent iron intermediates in

(51) Nam, W.; Ho, R. Y. N.; Valentine, J. S. *J. Am. Chem. Soc.* **1991**, *113*, 7052–7054.
(52) Kaizer, J.; Klinker, E. J.; Oh, N. Y.; Rohde, J.-U.; Song, W. J.; Stubna, A.; Kim, J.; Münck, E.; Nam, W.; Que, L., Jr. *J. Am. Chem. Soc.* **2004**, *126*, 472–473.
(53) Sastri, C. V.; Lee, J.; Oh, K.; Lee, Y. J.; Lee, J.; Jackson, T. A.; Ray, K.; Hirao, H.; Shin, W.; Halfen, J. A.; Kim, J.; Que, L., Jr.; Shaik, S.; Nam, W. *Proc. Natl. Acad. Sci. U.S.A.* **2007**, *104*, 19181–19186.
(54) Klinker, E. J.; Shaik, S.; Hirao, H.; Que, L., Jr. *Angew. Chem., Int. Ed.* **2009**, *48*, 1291–1295.
(55) Fiedler, A. T.; Que, L., Jr. *Inorg. Chem.* **2009**, *48*, 11038–11047.
(56) Yin, G.; Danby, A. M.; Kitko, D.; Carter, J. D.; Scheper, W. M.; Busch, D. H. *J. Am. Chem. Soc.* **2007**, *129*, 1512–1513.
(57) Yin, G.; Danby, A. M.; Kitko, D.; Carter, J. D.; Scheper, W. M.; Busch, D. H. *J. Am. Chem. Soc.* **2008**, *130*, 16245–16253.
(58) Chattopadhyay, S.; Geiger, R. A.; Yin, G.; Busch, D. H.; Jackson, T. A. *Inorg. Chem.* **2010**, *49*, 7530–7535.

the reaction of H_2O_2 with an iron(II) complex supported by a tetradentate bispidine ligand and found the formation of the corresponding dihydroxoiron(IV) species to be energetically quite facile, which they suggested may be the olefin *cis*-dihydroxylation agent in their catalytic system. Although no DFT calculations have been carried out on the Fe^{II}(R-DPAH) catalysts, these other studies support the mechanistic ideas we have developed in Scheme 2 on the basis of our experimental results.

In summary, we have explored the oxidation chemistry of iron complexes coordinated with bio-inspired facially oriented *N,N,O* ligands and found them to be effective catalysts for olefin *cis*-dihydroxylation with limiting H_2O_2 oxidant. These complexes show a significant improvement in oxidative efficiency and *cis*-dihydroxylation selectivity over the previously developed iron-based olefin *cis*-dihydroxylation catalysts that use H_2O_2 as the oxidant.[20] A mechanism is presented in Scheme 2 that can rationalize three important features of this catalytic system: (a) the strong preference for olefin *cis*-dihydroxylation over epoxidation with very high stereoretention, (b) the predominant incorporation of both oxygen atoms of H_2O_2 into the *cis*-diol product, and (c) the involvement of a water scrambling pathway competitive with olefin oxidation. These features are most easily accounted for by invoking the formation of an *fac*-(L)$Fe^{II}(\eta^2$-$H_2O_2)$(solv) adduct that forms a *fac*-(L)$Fe^{IV}(OH)_2$(solv) oxidant, which allows label scrambling to occur in the presence of $H_2{}^{18}O$. This is the first example of an iron-based *cis*-dihydroxylation catalyst for which experimental evidence for an Fe^{II}/Fe^{IV} redox cycle has been obtained. The insights derived from this work differ significantly from those reported in a very recent paper in which an oxoiron(V) species is implicated as the oxidant generated by the reaction of a *cis*-dichloroiron(III) complex of a macrocyclic tetraaza ligand with oxone; in this system, catalytic olefin *cis*-dihydroxylation can be achieved in high yield with a limiting substrate and a 2-fold excess of the oxone oxidant.[59] Taken together, these two catalytic systems demonstrate the versatility of high-valent iron in carrying out olefin *cis*-dihydroxylation. Our ongoing efforts are aimed at extending the lifetime of the R-DPAH catalysts and identifying reaction conditions that allow the Fe/H_2O_2 *cis*-dihydroxylation chemistry described here to be used in synthetic applications.

Acknowledgment. This work was supported by the United States Department of Energy (DE-FG02-03ER15455). We thank Dr. Victor G. Young, Jr. of the X-ray Crystallographic Laboratory at the University of Minnesota for invaluable assistance and Prof. William Tolman for the use of his Thermo Nicolet Avatar 370 FT-IR instrument.

Supporting Information Available: Tables S1 and S2 containing crystallographic data for **2** and **3**, Table S3 listing additional oxidation results, Figures S1 and S2 showing ESI-MS data of **2**−**5** and decomposed ligand, and Figure S3 showing results from an attempted Hammett correlation in the *cis*-dihydroxylation of styrenes. This material is available free of charge via the Internet at http://pubs.acs.org.

JA1021014

(59) Chow, T. W.-S.; Wong, E. L.-M.; Guo, Z.; Liu, Y.; Huang, J.-S.; Che, C.-M. *J. Am. Chem. Soc.* **2010**, *132*, 13229–13239.